Korean J. Chem. Eng., 33(6), 1917-1921 (2016)
DOI: 10.1007/s11814-016-0014-9

pISSN: 0256-1115
eISSN: 1975-7220

Bulk phase behavior of tetra-*n*-butylammonium bromide hydrates formed with carbon dioxide or methane gas

Sanehiro Muromachi†, Yoshitaka Yamamoto, and Satoshi Takeya

National Institute of Advanced Industrial Science and Technology (AIST), 16-1, Onogawa, Tsukuba 305-8569, Japan
(*Received 30 November 2015 • accepted 11 January 2016*)

Abstract−We report the bulk phase behavior of ionic clathrate hydrates of tetra-*n*-butylammonium bromide (TBAB) formed with a common guest substance: CO_2 or CH_4. We formed the bulk samples by a classical mixing reactor for gas hydrates, and measured them by the powder X-ray diffraction (PXRD). PXRD patterns of the TBAB+(CO_2 or CH_4) hydrates formed with 0.32 of TBAB mass fraction in the aqueous phase were obtained. They are consistent with the orthorhombic hydrate (Shimada et al., *Acta Crystallogr.* 2005; Muromachi et al., *Chem. Commun.* 2014), but not identical with the other stable phase, i.e., the tetragonal TBAB hydrate (Rodionova et al., *J. Phys. Chem. B* 2013). When the aqueous solutions are under the substantial pressure of CO_2 or CH_4 gas, TBAB is likely to form the orthorhombic *Pmma* and/or *Imma* phases. A question for the bulk orthorhombic TBAB hydrate phase about the scarce gas incorporation is newly proposed.

Keywords: Ionic Clathrate Hydrate, Carbon Dioxide, Methane, Tetra-*n*-butylammonium Bromide, Powder X-ray Diffraction

INTRODUCTION

Ionic clathrate hydrates, which are candidate materials for gas capture and storage, can form at mild temperatures, such as ~300 K, compared to canonical clathrate hydrates which generally require formation temperatures around 270 K. Small guest gases, such as N_2, CO_2, CH_4 and H_2, can be incorporated in the ionic clathrate hydrate structures, although they can form without guest gas [1-7]. Ionic guest substances, such as widely used tetra-*n*-butylammonium bromide (TBAB), are necessary to form the structure. In the quaternary ammonium and phosphonium salt hydrate structures, the guest cation is included in the four cage-fused cage, and the guest anion makes hydrogen bonds with the water molecules surrounding the guest cation [8-12]. Particularly with the halogenated TBA salts, several hydrate structures can form even with the same ionic guest substance due to a couple of possible packings of the TBA cation [10,13,14]. This polymorphism may be a problem in the applications of the hydrates: If a hydrate phase with a low gas capacity accidently forms, the system performance should drop enormously. Therefore, analysis and controlling methods of the hydrate phases are necessary.

The polymorphism of the TBAB hydrates was first detailed by Gaponenko et al. [13], who reported that TBAB can form four different hydrate phases. Oyama et al. reported the phase equilibrium data in the system in which two dominant TBAB hydrate phases coexisted at temperatures from 273 to 285 K, i.e., orthorhombic phase with the hydration number of 38 and tetragonal phase with the hydration number of 26 [15]. The crystal structure model of the orthorhombic TBAB hydrate with *Pmma* space group was determined by Shimada et al. [11] Rodionova et al. [16] tried to solve the tetragonal TBAB hydrate structure, but it was yet-to be solved probably due to its poor crystallinity. In this decade, ionic clathrate hydrates were considered to have potential for gas storage, transportation and separation applications; however, due to the above-mentioned polymorphism and complexity of the ionic guest structure, it was difficult to characterize these materials. Lee et al. [3] analyzed the TBAB+(CH_4 or CO_2) hydrates through the nuclear magnetic resonance (NMR) and Raman spectroscopic techniques. Jin et al. [17] found that a phase transition of TBAB+Xe gas hydrates occurs depending on the pressure. Recently, we performed single crystal X-ray structure analyses on the TBAB+CO_2 hydrates [18]. Interestingly, the TBAB+CO_2 hydrates have a similar but transformed orthorhombic hydrate structure induced from the guest CO_2. We reported phase equilibrium data for the TBAB+N_2 hydrates, which showed the two different pressure-temperature slopes [6]. According to the single crystal X-ray diffraction analyses, the orthorhombic hydrate phases are formed in the conditions near the two different pressure-temperature slopes. It was suggested that the slope change occurred by N_2 gas incorporation rather than by a hydrate structure change such as tetragonal phase to orthorhombic phase. These results obtained by the single crystal structure analyses suggested the polymorphism of the TBAB+gas hydrates, as well as the TBAB hydrates without guest gas. Accordingly, it is necessary to investigate their properties, such as crystal structure and guest gas capacity, of the bulk sample synthesized in a practical formation reactor, e.g., in which the liquid, gas and hydrate phases are well mixed.

We report here the bulk phase characterization of TBAB+(CO_2 or CH_4) hydrates using powder X-ray diffraction (PXRD) measurements. The bulky samples of TBAB hydrates containing guest

†To whom correspondence should be addressed.
E-mail: s-muromachi@aist.go.jp

CO_2 or CH_4 gas were formed with a classical gas hydrate-formation reactor, which had a low aspect ratio of height to inner diameter, and was equipped with a stirrer. The PXRD patterns of the formed bulk samples were compared with the previously reported crystal structure models determined by the single crystal structure analysis. The comparison revealed that the samples formed with the guest gas were the orthorhombic TBAB hydrates. We also performed the PXRD measurement for the tetragonal TBAB hydrate, which was obtained as a form of single crystal. It was confirmed that the TBAB+(CO_2 or CH_4) hydrate samples formed in the conventional stirring reactor consisted of the orthorhombic phase.

EXPERIMENTAL

1. Materials

We used deionized and distilled water. Specifications of tetra-*n*-butylammonium bromide (TBAB) and guest gases are summarized in Table 1. We directly used these materials as received from their respective manufacturers.

2. Hydrate Sample Preparation

We formed four TBAB hydrate samples as listed in Table 2. To form samples 1-3 which were formed with guest gas, we used a high pressure cell. Sample 4 was formed without guest gas using another apparatus.

A schematic diagram of the formation apparatus for samples 1-3 is shown in Fig. 1. The apparatus mainly consists of a stainless-steel high pressure cell, an aqueous ethylene glycol bath, a PID (Proportional-integral-derivative) controlled heater, an immersion cooler, and a data logger. The cell had a thermometer, a magnet induced stirrer and a pressure sensor. The dimension of the inner space of the cell was 80 mm-diameter and 40 mm-height, and its volume was approximately 200 cm^3. The stirrer was equipped with two agitating blades. We gravimetrically prepared the aqueous TBAB solutions with the prescribed concentrations. After we injected ~30 g of the sample solutions into the cell, it was moved to the bath. To eliminate residual air in the cell, we repeated the following process three times: Vacuumed the cell up to ~5 kPa and charged the cell

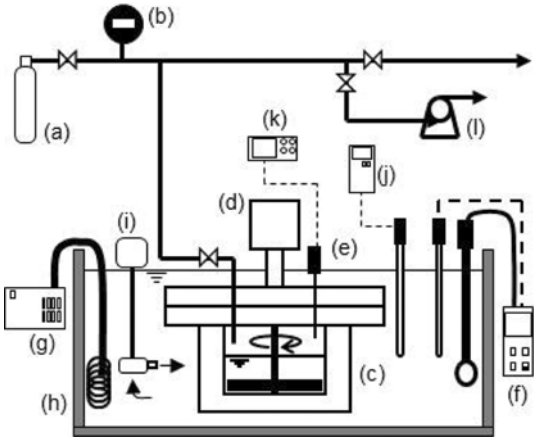

Fig. 1. Schematic diagram of the gas hydrate formation apparatus.

(a) Gas cylinder	(g) Cooler
(b) Pressure monitor	(h) Water bath
(c) High pressure cell	(i) Jet pump
(d) Magnetic stirrer	(j) Thermometer
(e) Pressure sensor	(k) Data logger
(f) PID controlled heater	(*l*) Vacuum pump

with the gas, i.e., methane or carbon dioxide with 1 MPa. Subsequently, we supplied the gas to the cell with the pressure shown in Table 1. The formation conditions were also shown on the pressure-temperature plane (Fig. 2) The subcooling degree of the temperature was ~2.5 K in each case.

The cell temperature was maintained until the pressure decrease stopped. After that, we cooled the cell to the ~220 K by immersion in liquid nitrogen. The cell was discharged with the gas and opened, and the hydrate sample was preserved in a refrigerator of which temperature was maintained at < 140 K.

The TBAB hydrates formed without gas (sample 4) were synthesized in the other apparatus. The apparatus consists of a water bath made of polymethyl methacrylate, a cooling water circulator and a thermometer, and it was basically the same as that used in our previous studies [12,19]. The aqueous solution of TBAB was

Table 1. List of materials used in this study

Name	Chemical formula	Supplier	Purity
Carbon dioxide	CO_2	Taiyo Nippon Sanso, Co., Tokyo, Japan	≥0.99995 in mol fraction
Methane	CH_4	Tokyo Gas Chemicals Co., Ltd., Japan	≥0.999999 in mole fraction
Tetra-*n*-butylammonium bromide	$(n\text{-}C_4H_9)_4NBr$	Sigma-Aldrich, Co.	≥0.99 in mass fraction

Table 2. TBAB hydrate samples formed in this study

Sample number	Concentration of TBAB in aqueous solution/mass fraction	Guest gas	Formation temperature/K	Initial pressure /MPa
1	0.320	CO_2	288.2	3.1[a]
2	0.100	CO_2	285.8	3.1
3	0.320	CH_4	288.2	2.98
4	0.300[b]	Not used	283.2	

[a]The formation pressure for sample 1 was recharged again after once the formation ceased

[b]After single crystals grew, they were separated from the aqueous phase

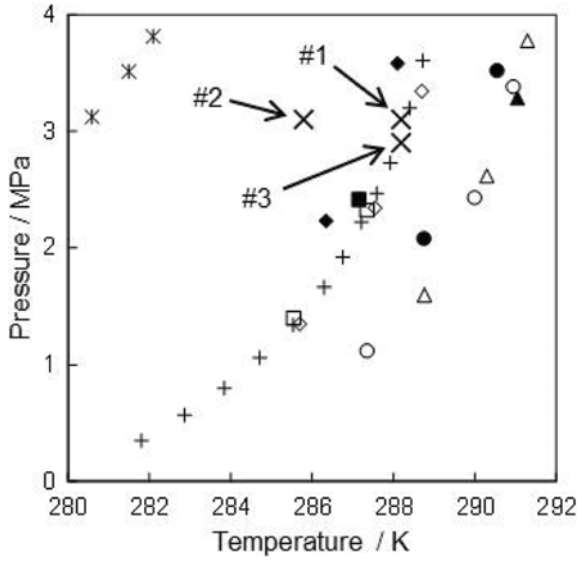

Fig. 2. The formation conditions of the TBAB+(CH_4 or CO_2) hydrates. ×, the PXRD samples in this study; ◇, TBAB+CO_2 hydrate, w=0.097, x=0.006 [3]; ○, TBAB+CO_2 hydrate, w=0.407, x=0.037 [3]; □, TBAB+CO_2 hydrate, w=0.1, x=0.006 [2]; +, TBAB+CO_2 hydrate, w=0.1, x=0.006 [5]; △, TBAB+CO_2 hydrate, w=0.32, x=0.026 [5]; ◆, TBAB+CH_4 hydrate, w=0.1, x=0.006 [3]; ●, TBAB+CH_4 hydrate, w=0.41, x=0.037 [3]; ■, TBAB +CH_4 hydrate, w=0.1, x=0.006 [2]; ▲, TBAB+CH_4 hydrate, w=0.3, x=0.023 [2]; ✳, CO_2 hydrate [21]. Here the "w" and "x" denote the mass fraction and mole fraction of TBAB in the aqueous phase, respectively.

injected into a glass vial and it was set in the bath. The bath temperature was maintained at 283.2 K during the crystal growth. At this temperature, only the tetragonal TBAB hydrate can form according to the phase diagram reported by Oyama et al. [15]. We sampled the crystals from the vial, and kept them at 96 K in the subsequent processes.

The measurement uncertainties were 0.2 K for temperature, 0.05 MPa for pressure and 0.005 for TBAB mass fraction in the aqueous phase, respectively.

3. Powder X-ray Diffraction Measurements

PXRD measurements were performed in the $\theta/2\theta$ step scan mode using Cu Kα radiation (wave length: 1.541 Å) with a step width of 0.02° in the 2θ. Count time per step was 8.0 s for the TBAB+(CO_2 or CH_4) hydrates, but the time for the TBAB hydrate was 15.0 s so as to obtain a similar background signal-to-noise (SN) ratio of PXRD pattern to those of TBAB+(CO_2 or CH_4) hydrates. LaB_6 (NIST) was used as an external standard to determine a 2θ angle offset of parallel beam optics (40 kV, 40 mA; Rigaku model Ultima III). To perform the measurements for the samples, they were finely-powdered and mounted on a copper PXRD sample holder under nitrogen gas below 100 K. The analysis of the unit-cell parameters was performed by a whole-pattern fitting method in the 2θ range of 6-50° using the Rietveld program RIETAN-FP [20].

RESULTS AND DISCUSSION

During the formation of samples 1-3, the gas uptake by the gas hydrate formation ceased with a very low conversion ratio of gas hydrate. In each case of samples 1-3, the pressure drops due to the hydrate formation were a few hundreds kPa, which was quite lower than the stoichiometric gas capacity, i.e., 38 NL(CO_2)/kg(TBAB+CO_2 hydrate) determined by single crystal XRD diffraction analysis. We recharged the cell up to the initial pressure after the first system pressure drop ceased; however, further gas uptake was not observed. Such little gas uptake is often reported for the gas containing ionic clathrate hydrate [4,22,23], while the structure model determined by the single crystal XRD [18] indicated a sufficient CO_2 occupancy as much as the cubic structure I hydrate.

Fig. 3 shows a comparison of PXRD pattern between the structure models of the TBAB hydrate and the TBAB+CO_2 hydrate, both of which have the orthorhombic lattice. These PXRD patterns were simulated according to crystal structures analyzed by single crystal structure method in earlier studies [11,18], and the difference between these patterns can be seen at 2θ angles below ~15°.

Fig. 3 together shows the PXRD patterns of Samples 1-4 formed

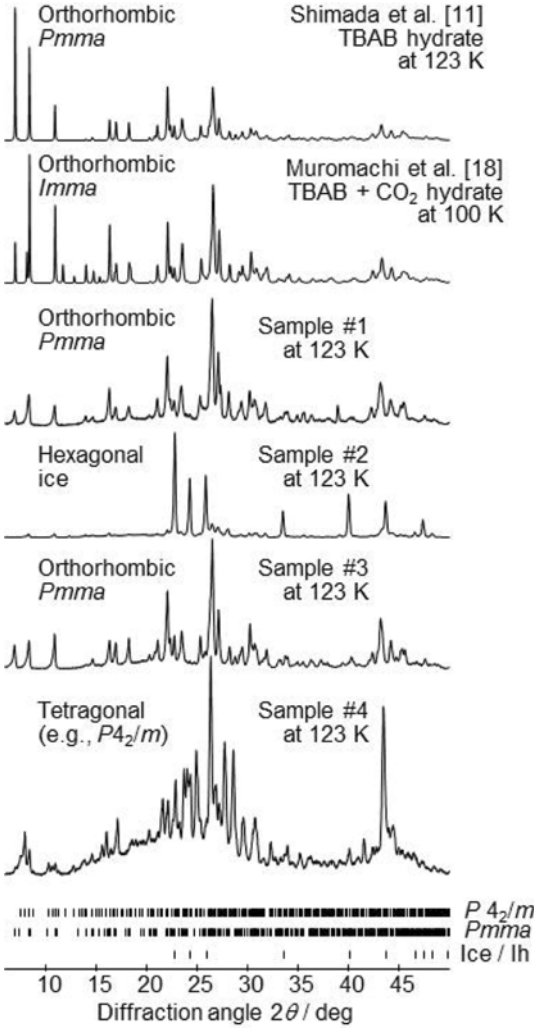

Fig. 3. PXRD patterns of the TBAB hydrates: Structure models from the references [11,18] and samples formed in this study. Sample 2 mainly consists of the hexagonal ice phase with small amount of TBAB hydrate.

in this study. Sample 1 shows an orthorhombic pattern (a=21.064(3), b=12.635(2), c=12.043(2) Å) similar to the orthorhombic TBAB hydrate (a=21.060(5), b=12.643(4), c=12.018(8) Å with space group: *Pmma* at 93.1 K) [11]. Here, any apparent diffraction peaks from hexagonal ice (Ih) phase were not observed in sample 1, which means that the quench process used in this study is enough slow to form the TBAB hydrates rather to form the TBAB solid and Ih phases separately. Contrary to this, sample 2 mainly consists of Ih phase with a little of the TBAB hydrate. The cubic structure I clathrate hydrate which is formed by CO_2 without TBAB, was not observed in sample 2.

Sample 3 also shows an orthorhombic pattern (a=21.056(2), b=12.618(1), c=12.047(1) Å) similar to the orthorhombic TBAB hydrate as well as sample 1. Any significant difference between the patterns of samples 1 (TBAB+CO_2) and 3 (TBAB+CH_4) cannot be found. Both samples 1 and 3 consisted of only the orthorhombic hydrate phase, though the guest gas uptake during the formation processes was not enough. These results showed that the guest CO_2 and CH_4 gases can induce the formation of the orthorhombic phase, because that has the largest potential gas capacity among the TBAB hydrate structures [18]. The present results significantly regard with our previous study [6]: the two different orthorhombic crystals of the TBAB+N_2 hydrates, i.e., high and low gas content crystals, formed depending on the pressure range. Therefore, other analytical techniques, such as nuclear magnetic resonance and Raman spectroscopy, may be useful for estimating the amount of incorporated guest gases (cage occupancies) in these hydrate structures.

The tetragonal TBAB hydrate, Sample 4, was obtained as a form of single crystals. Fig. 4 shows the tetragonal TBAB hydrate crystals. The crystal shape is squared column, and clearly different from those of the orthorhombic TBA salt hydrates observed in the previous studies, which were the hexagonal columnar shape [5,6,12].

In Fig. 3, the PXRD pattern of Sample 4, especially the peaks at $2\theta<15^{o}$, was different from the others. The peak pattern can be indexed by a tetragonal phase (a=23.487(3), c=12.555(3) Å) such as the yet-to-refined crystal structure of tetragonal $P4_2/m$ [16]. In this figure, the pattern of Sample 4 is clearly different from that of the others, which means that Sample 4 has a different TBAB hydrate phase. Here, also, Sample 4 has a broader and larger PXRD background intensity than the other TBAB hydrates. This might suggest that the sample contains amorphous-like phases, but further experiments and analyses are necessary to discuss the occurrence of the amorphous-like phases.

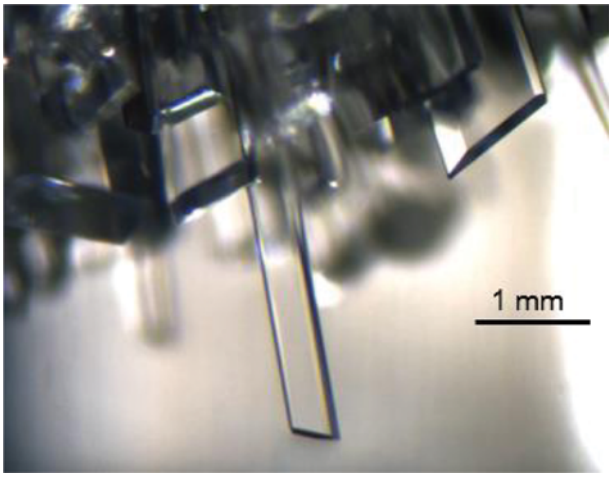

Fig. 4. Photograph of sample 4: Single crystals of the tetragonal TBAB hydrate formed without a gas.

CONCLUSION

We report the PXRD patterns of the TBAB hydrate samples which formed with CO_2 or CH_4 gas in the classical gas hydrate reactor. The obtained PXRD patterns are compared with the structure models of the TBAB hydrates with orthorhombic *Pmma* phase and the TBAB+CO_2 hydrate with orthorhombic *Imma* phase. The TBAB+CO_2 or CH_4 hydrates formed with 0.32 of TBAB mass fraction in the aqueous phase are consistent with the orthorhombic hydrate model. The tetragonal TBAB hydrate sample formed without guest gas showed an evidently different PXRD pattern from that of the orthorhombic *Pmma* and *Imma* phases.

We dealt with the issue of the practical formation of the TBAB hydrates: which phase forms during the bulk formation. The bulk samples of the TBAB+(CO_2 or CH_4) hydrates consisted of a single phase, and were mostly identical to the single crystals formed in previous studies. Therefore, TBAB may only form the orthorhombic *Pmma* and/or *Imma* phases, when the aqueous solutions are under the substantial pressure of CO_2 or CH_4 gas. This is mainly because the orthorhombic hydrate phase has the most efficient gas capacity, i.e., the ratio of the number of dodecahedral cages to that of water molecules in the structure is the largest among the possible hydrate structures. These results were consistent with our previous study, in which the two different orthorhombic TBAB hydrate crystals formed, depending on the N_2 pressure. A new question for the bulk orthorhombic TBAB hydrate phase about the scarce gas incorporation arises.

ACKNOWLEDGEMENT

SM received a Grant-in-Aid for Young Scientists (B) from the Ministry of Education, Culture, Sports, Science, and Technology of Japan (No. 26820069).

LIST OF SYMBOLS

θ : X-ray diffraction angle in the Bragg law.
a : Lattice constant along a axis
b : Lattice constant along b axis
c : Lattice constant along c axis
w : TBAB mass fraction in the aqueous phase
x : TBAB mole fraction in the aqueous phase

REFERENCES

1. A. Chapoy, R. Anderson and B. Tohidi, *J. Am. Chem. Soc.*, **129**, 746 (2007).
2. M. Arjmandi, A. Chapoy and B. Tohidi, *J. Chem. Eng. Data*, **52**,

2153 (2007).
3. S. Lee, S. Park, Y. Lee, J. Lee, H. Lee and Y. Seo, *Langmuir*, **27**, 10597 (2011).
4. D. Zhong and P. Englezos, *Energy Fuels*, **26**, 2098 (2012).
5. N. Ye and P. Zhang, *J. Chem. Eng. Data*, **57**, 1557 (2012).
6. S. Muromachi, H. Hashimoto, T. Maekawa, S. Takeya and Y. Yamamoto, *Fluid Phase Equilib.*, **413**, 249 (2016).
7. P. Babu, W. I. Chin, R. Kumar and P. Linga, *Ind. Eng. Chem. Res.*, **53**, 4878 (2014).
8. G. A. Jeffrey, in *Inclusion Compounds*, (Eds. J. L. Atwood, J. E. D. Davies and D. D. MacNicol), Academic Press: London, Vol. 1, Chapter 5 (1984).
9. D. W. Davidson, in *Water. A Comprehensive Treatise*, (Ed. F. Franks), Plenum Press, New York, NY (1973).
10. Y. A. Dyadin and K. A. Udachin, *J. Struct. Chem.*, **28**, 75 (1987).
11. W. Shimada, M. Shiro, H. Kondo, S. Takeya, H. Oyama, T. Ebinuma and H. Narita, *Acta Crystallogr.*, **C61**, o65 (2005).
12. S. Muromachi, S. Takeya, Y. Yamamoto and R. Ohmura, *CrystEngComm*, **16**, 2056 (2014).
13. L. A. Gaponenko, S. F Solodovnikov, Y. A. Dyadin, L. S. Aladko and T. M. Polyanskaya, *J. Struct. Chem.*, **25**, 175 (1984).
14. T. Kobori, S. Muromachi, T. Yamasaki, S. Takeya, Y. Yamamoto, S. Alavi and R. Ohmura, *Cryst. Growth Des.*, **15**, 3862 (2015).
15. H. Oyama, W. Shimada, T. Ebinuma, Y. Kamata, S. Takeya, T. Uchida, J. Nagao and H. Narita, *Fluid Phase Equilib.*, **234**, 131 (2005).
16. T. V. Rodionova, V. Y. Komarov, G. V. Villevald, T. D. Karpova, N. V. Kuratieva and A. Y. Manakov, *J. Phys. Chem. B*, **117**, 10677 (2013).
17. Y. Jin and J. Nagao, *J. Phys. Chem. C*, **117**, 6924 (2013).
18. S. Muromachi, K. A. Udachin, K. Shin, S. Alavi, I. L. Moudrakovski, R. Ohmura and J. A. Ripmeester, *Chem. Commun.*, **50**, 11476 (2014).
19. S. Muromachi, M. Kida, S. Takeya, Y. Yamamoto and R. Ohmura, *Can. J. Chem.*, **93**, 954 (2015).
20. F. Izumi and K. Momma, *Solid State Phenom.*, **130**, 15 (2007).
21. S. Adisasmito, R. J. Frank and E. D. Sloan, *J. Chem. Eng. Data*, **36**, 68 (1991).
22. N. Ye, P. Zhang and Q. S. Liu, *Ind. Eng. Chem. Res.*, **53**, 10249 (2014).
23. J. Sangwai and L. Oellrich, *Fluid Phase Equilib.*, **367**, 95 (2014).